Available online at www.sciencedirect.com

ScienceDirect

Procedia CIRP 88 (2020) 411–416

www.elsevier.com/locate/procedia

13th CIRP Conference on Intelligent Computation in Manufacturing Engineering, CIRP ICME '19

Ti-6Al-4V lattice structures produced by EBM: Heat treatment and mechanical properties

Manuela Galati[a,*], Abdollah Saboori[b], Sara Biamino[b], Flaviana Calignano[a], Mariangela Lombardi[b], Giovanni Marchiandi[a], Paolo Minetola[a], Paolo Fino[b], Luca Iuliano[a]

[a] *Department of Management and Production Engineering (DIGEP), Politecnico Di Torino, Corso Duca degli Abruzzi 24, 10129 Torino, Italy*
[b] *Department of Applied Science and Technology (DISAT), Politecnico Di Torino, Corso Duca degli Abruzzi 24, 10129, Torino, Italy*

* Corresponding author. Tel.: +390110907280; *E-mail address:* manuela.galati@polito.it

Abstract

Additive manufacturing (AM) processes allow producing the complex components in a layerwise fashion. The complexity includes the design of lighter and stronger components by using lattice structures that can be quickly realized through AM technologies. However, the mechanical behaviour of lattice structures is not completely known, especially in the post-treated state. Thus, this work aims to explore the effect of post-treatment on the compressive strength of specimens with lattice structures. The samples are produced using Ti-6Al-4V powder processed by Electron Beam Melting (EBM). The outcomes of this work confirm the correlation between the heat treatment and final mechanical properties.

Peer review under the responsibility of the scientific committee of the 13th CIRP Conference on Intelligent Computation in Manufacturing Engineering, 17-19 July 2019, Gulf of Naples, Italy.

Keywords: Additive manufacturing; Electron beam melting; lattice structure; Ti-6Al-4V; Mechanical properties; Heat treatment

1. Introduction

Additive Manufacturing (AM) is defined as "a process of joining materials to make objects from 3D model data, usually layer upon layer, as opposed to subtractive manufacturing methodologies"[1, 2]. This kind of approach allows the production of parts with free design constrains enabling the construction of integrated parts, lightweight structures or topologically optimized [3]. At the industrial level from the beginning of the 21st century, there has been an increment of interest in AM due to the large production flexibility of this technologies, both on the cost and lead-times. In the last few years, the industrial sector interest has been significantly focused on metal AM techniques for aerospace, automotive and medical applications. For aerospace and automotive, the main drivers for the AM introduction as a production technique is the possibility to obtain lightweight components and integrated parts [3]. For medical, instead, the main driver is the possibility to obtain personalized implants which allow the reduction of the recovery times, due to the better interaction with prior tissues [4]. Among the metal AM techniques, a great interest has developed around the Electron Beam Melting (EBM) process which is today already used for mass production in aerospace and medical applications. The EBM process is based on the selective melting of metallic powder using an electron beam. Arcam has developed the first EBM system [5] in 1987, and to date, it is still the only manufacturer for the EBM systems around the world. Different materials can be processed by EBM technology, such as stainless steels, tool steels, Co-based superalloys, Ni-based superalloys and most importantly Ti-alloys or the intermetallic TiAl [6]. Among the Ti-alloys, Ti-6Al-4V alloy is largely used to produce parts by EBM because of its capacity to overcome the limitations of the traditional melting techniques [7] due to the need to remove high density inclusions (HDI) as well as low density inclusions (LDI) to provide composition homogeneity [8] and avoid the surface oxidation, especially at high temperatures. In fact, the EBM process works in a vacuum environment and at high temperatures due to the preheating step that precedes the

2212-8271
Peer review under the responsibility of the scientific committee of the 13th CIRP Conference on Intelligent Computation in Manufacturing Engineering, 17-19 July 2019, Gulf of Naples, Italy.
10.1016/j.procir.2020.05.071

melting step [7]. In the work chamber, in fact, the achieved temperature is approximately the preheating temperature (650-700°C for Ti-6Al-4V). This aspect ensures small thermal shrinkages and a high grade of consistency of the non-melted powder which acquires a certain strength [9]. For this reason, the EBM process requires a small amount of supports and allows the building of the micro-architectured materials to be produced easily without using support structure. Micro-architectured materials also called cellular materials had been largely addressed because the possibility to achieve a unique combination of properties [10]. Among the cellular materials, foams and lattice structures randomly have proved to exhibit extremely excellent properties with respect to the corresponding bulk material [11]. Jointly to the use of Ti-6Al-4V, these structures made by EBM showed interesting properties such as specific strength [12], oxidation resistance [12, 13] and biocompatibility with human tissues [13, 14]. Ashby [15] identified three main factors that influence properties of cellular solids; 1) material of which is made, 2) cell topology and shape, 3) relative density. The first factor affects the mechanical, the thermal and the electrical properties. Cell topology and shape are important for the behaviour distinction between bending and stretching-dominated structures. The relative density affects the properties of cellular solids. The relative density [16] is calculated by the ratio between the density of cellular material ρ^* and the density of the bulk material ρ_s. Ashby and Gibson [16] proposed a model for cellular solids that connects a generic relative property with the relative density using a logarithmic law. The main drive for the design of foams is relative density, while the design of lattice structures is driven even by the topology and dimensions of the unit cell. Differently from foams, lattice structures also called cellular, reticulated or truss structures are defined as structures made up of a large number of uniform elements and generated by tessellating a unit cell throughout space [10]. Since the lattice properties are strongly design-dependent, several studies have been addressed to investigate the macroscopic properties for different geometries. Cansizoglu et al. [17] evaluated the behaviour of the honeycomb lattice structures with different strut sizes. Heinl et al. [18] studied cross and diamond unit cells with interconnected macro porosity made by EBM for bone implants applications. Diamond lattice structures with graded porosity have been analyzed by van Grunsven et al. [19]. Jamshidinia et al. [20] studied lattice structures for specific dental implant applications. Three different unit cells (cross, honeycomb and octahedral) with different cell sizes were investigated with the aim to provide a dental abutment with specific elastic micro-motion. The compression behaviour of open-cell rhombic dodecahedron structure with two configurations of strut size ratio l/d and under different work temperatures has been investigated by Xiao et al [28]. [21]. Li et al. [22] investigated the compression fatigue behaviour at different load levels of rhombic dodecahedron unit cells lattice structures with a range of density between 0.73 and 1.68 g/cm^3. All studies analysed mechanical behaviour of lattice structures using compression tests.

At the room temperature, nominal stress-strain curves of lattice structures under uniaxial compression show three distinguishing parts: 1) the elastic behaviour of the lattice structure, 2) a progressive collapse of the layers up to the structure has 3) the same behaviour of the bulk material — the failure of the specimens typical at 45° by brittle fracture. Larger cell size showed worse performances than smaller cell size, in terms of both elastic modulus and collapse strength. As far as the microstructure is concerned, in contrast with bulk material, the microstructure of the mesh arrays is α'-martensite phase. The microstructure developments and differences between the bulk material and the cellular materials have been investigated by Murr et al. [23] While acicular α-phase and β-phase were presented in the bulk material, the microstructure of a cellular material with a strut size of 1.1 mm was a fine mixture of α, α'-martensite and β-phase grains. Increasing the strut size, an increase in Widmanstatten α+β phases was found [24]. The difference between the microstructure of bulk and any cellular materials is due to the different cooling rates in the air gaps [12]. As well known, the microstructure of the material as well as its mechanical performance can be modified by subsequent heat treatments. For Ti-6Al-4V parts produced by EBM technology, heat treatments are very common, but in parts that could contain micro porosity, treatments such as annealing could cause a growth of the pores [25]. For such small structures as in the case of lattice structures, an internal defect due to residual porosity in the powder bed or high surface roughness plays a key role in the mechanical resistance [26]. However, only one study in literature addressed this aspect evaluating the effect of defects on the mechanical response of Ti-6Al-4V cubic lattice structure [27]. Two annealing treatments were run at a lower temperature than β-transus (960°C) and a higher one than β-transus (1200°C), respectively. Both were conducted for a total time of 120 minutes, and air pressure. For the as-built condition the microstructure of the struts perpendicular to the start plate showed a combination of α and β phases, according to previous studies on the bulk material [23, 28, 29]. For the temperature lower than β-transus annealing, no consistent differences were found with respect to the as-built microstructure. For the temperature condition higher than β -transus annealing, a coarsening of the microstructure was detected. For that, the mechanical tests showed a lower compressive yield stress by approximately 11%. To fill that gap, the presented work addressed the effect of design and heat treatment on the compression behavior of lattice structure. A lattice structure was designed and produced in different sizes by using an Arcam A2X. An annealing heat treatment was run at a temperature higher than β-transus (1050°C) for 60 min with subsequent furnace cooling. As-built and treated specimens were tested under compression. Three replications for each test have been carried out.

2. Experiments

2.1. Lattice Design

The elementary cell chosen for this study is a dodecahedral cell (Fig.1a). The lattice structure was designed using Magics 21.11. The cell was repeated in a cylindrical volume of

diameter 20 mm and height 26 mm. The cell was used in three different sizes equal to 4 mm (Fig.1b), 7 mm (Fig.1c) and 10 mm (Fig. 1d), respectively. The minimum cross-section area depends on the cell size and it was about 4.85 mm^2, 3.85 mm^2 and 2.61 mm^2, respectively, for the cell size of 4 mm, 7 mm and 10 mm. The average area was calculated to be 12.326 mm^2, 12.562 mm^2 and 12.0418 mm^2 respectively for the cell size of 4 mm, 7 mm and 10 mm.

To have a uniform distribution of the load during the compression test, two discs of the same diameter of the lattice part and 2 mm thick are added at the bottom and the top of the lattice structure. The discs are a part of the specimen.

2.2. Design of Experiment and Production

To have a robust experimental analysis, for each size three replicas were produced. Therefore, 18 samples were realized to investigate the mechanical behavior of both as-built and treated lattice samples. The build job was designed using Magics 21.11. Moreover, bulk specimens were designed to evaluate the actual density of the Ti-6Al-4V made by EBM process. The standard themes provided by Arcam were used for the lattice volume and full melted parts (discs and bulk specimens). To avoid microstructure modifications, all specimens were produced unattached to the start plate. Fragile and think support structures with 20 mm height were used at the bottom of specimens to support them during their building on the powder layer. Additionally, to have a uniform temperature distribution during the process, the specimens were opportunely distributed along the building axis to have an almost constant melting area for each layer. The build job was processed by EBM build processor 5.0. The specimens were produced using an Arcam A2X system and standard Ti-6Al-4V powder (Fig. 2). As can be seen in Fig. 2, the starting powder is completely spherical, and no internal porosity was found in the cross-section of this powder. At the end of the process, the entire build was cooled down within the EBM chamber up to the environment temperature. Thereafter, the specimens were cleaned using a sandblasting process with the same powder used during the process and an air pressure equal to 4 bar. The cleaning procedure has been aimed to remove all residual powder.

2.3. Heat treatment and compression test

Nine specimens of the 18 produced were treated. The heat treatment experiment conducted in this study is a super β-transus treatment. In fact, during the heat treatment, the samples were heated to a peak temperature (1050 °C) with a heating rate of 5 °C/min and then soaked at temperature for 60 min and cooled at a constant rate in the furnace. The heat treatments were performed in a Vacuum furnace (Pro.Ba.) which can attain vacuum levels of 1e-5 mbar for annealing. Axial compression tests were carried out using Easydur Aura machine for both as-built and heat treated setting a strain rate equal to 2mm/min. The tests were run up to the failure of the specimens. Similar loads/displacements trends have been observed for the replicas with the same cell size. The stress/strain curves were evaluated from the load/displacement curves considering the area corresponding to the cross section of the cylinder specimen.

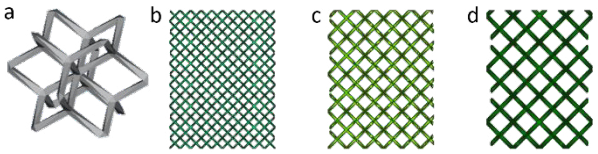

Fig.1 (a) Elementary cell; Specimen with elementary cell of size (b) 4 mm, (c) 7 mm and (d) 10 mm.

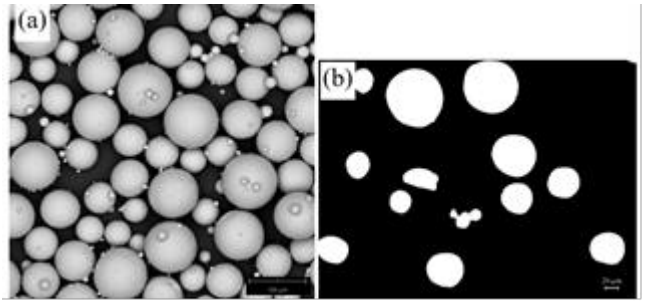

Fig. 2. (a) SEM image, (b) cross-section of starting Ti-6Al-4V powder.

2.4. Characterization

The relative densities for the lattice structures were calculated to 27.33%, 20.87% and 18.18%, respectively, for the cell size of 4 mm, 7 mm and 10 mm.

For microstructure observation, the samples were cut, mount ground, fine polished and then etched using Kroll's reagent (2%HF, 4% HNO_3 in water). Images were taken using the Leica optical microscope for the cross-section of powders and Phenom table-top Scanning Electron Microscope (SEM) for the microstructure of printed samples and morphology of powder.

3. Results and Discussion

3.1. Effect of the cell size

Fig. 3 shows a representative result of the compression tests carried out on the three replicas. As can be seen in this Figure, the general trend for all the trials for the cell size of 10 mm are rather similar and all the results were consistent.

As mentioned earlier, to evaluate the effect of cell size, three compression tests per each cell size were carried out. Fig. 4 shows the experimental stress-strain curves for the lattice specimens with three different cell sizes equal to 4 mm, 7 mm and 10 mm. From this figure, it is evident that by increasing the cell size the compressive strength of lattice samples decreases significantly. This significant difference in the compression behaviour of lattice is attributed to the increase of the relative density with the reduction of the unit cell size.

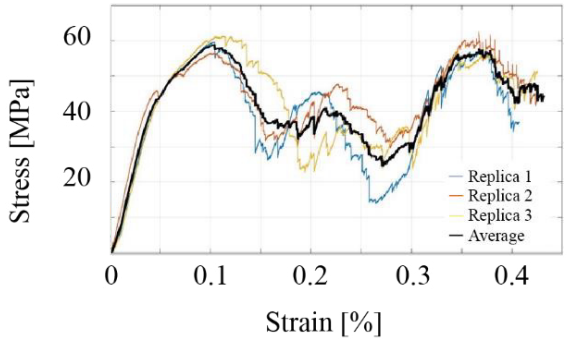

Fig. 3. Compressive deformation behavior of Ti-6Al-4V cellular structures in the as-built condition (size of the lattice 10 mm).

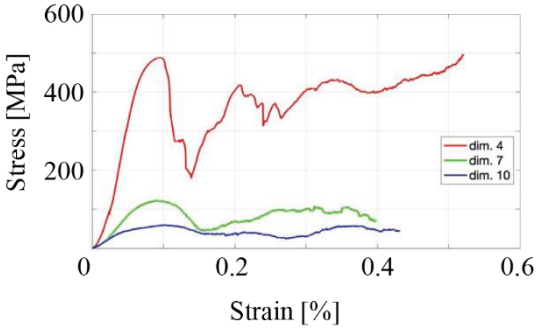

Fig. 4. Experimental stress-strain curves for the lattice specimens with three different cell sizes of 4 mm, 7 mm and 10 mm.

3.2. Effect of heat treatment

Fig. 5(a) shows the as-built microstructure of Ti-6Al-4V alloy produced by EBM which is lamellar, with fine α platelets oriented in various directions. Although some α colonies can be revealed that is indicative of a relatively fast cooling rate during the β to α phase transformation. Moreover, Figure 5 shows clearly that the microstructure of Ti-6Al-4V alloy is typical of any (α+β) alloy, i.e. the Widmanstätten α platelets of different sizes and orientations.

As mentioned earlier, the microstructure of Ti-6Al-4V alloy is typical of any (α+β) alloy and heat treatment induces coarser α lamellae (Fig. 5 (b)). Indeed, for the super β-transus heat treatments, the α phase is completely dissolved, and the final α morphology depended primarily on the cooling rate, which was constant for the furnace cooled tests in the current study. The impact of the microstructural condition on the mechanical performance can be revealed for all loading conditions. The compressive force-deformation behavior of as-built and as-heat treated samples are compared in Fig. 6. The graph of as-built lattice shows the typical behavior of brittle cellular materials at low degrees of deformation. From this figure, it can be noticed that, in general, the compressive behaviour of the heat-treated lattice seems to be similar to the as-built trend. However, the profile of each curve is different: it is possible to see a progressive trend approaching the ultimate compressive strength (UCS) and then an almost trend and then an almost constant trend, not characterized by the continuous drops and rises of the as-built sample. The trend seems to be smoother overall in the case of heat-treated samples. There is no significant variation in Young's modulus (*E*), as it is possible to see from the curves, but a slightly reduction of UCS is observable. Nonetheless, it is found that the compressive behaviour of the heat-treated sample seems to

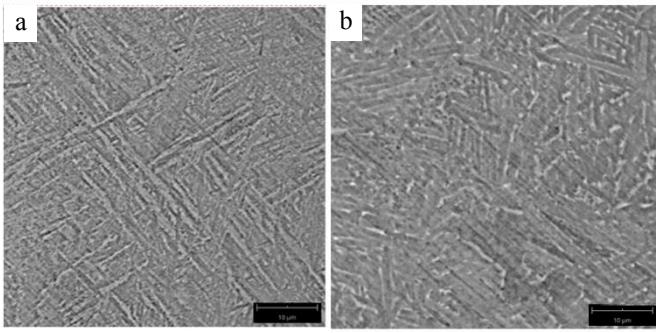

Fig. 5. SEM images of (a) as-built, (b) heat treated Ti-6Al-4V alloy.

be ductile instead of rather brittle behaviour in as-build condition. This discrepancy in the compression behaviour of heat treated and not-heat treated could be attributed to the α'-microstructure of as-built lattice that leads to a higher sensitivity to local defects.

Moreover, it is revealed that in comparison with the heat-treated samples, the as-built samples bear higher maximum stresses before a steep drop occurs at strains of about 6-7%. This drop is attributed to failure of struts along an entire plane of the cube and is deeper in case of the as-built sample revealing an inferior ductility. After this collapse both samples bear load again with higher maximum stresses present in the heat-treated sample.

Through the evaluating of Young's modulus and UCS from the curves and dividing them by E_0 and UCS_0, respectively, it is possible to evaluate relative properties. As shown by Ashby and Gibson, there is a relationship between relative properties of cellular solids and their relative density. Fig. 7 shows the relative mechanical characteristics of lattice before and after the heat treatment and their comparison with the Ashby-Gibson model.

Fig.7 depicts that only for higher relative density the as-built samples bear higher maximum relative stresses with respect to the heat-treated lattice while for the Young's modulus a higher value was obtained for heat-treated sample. Furthermore, it should be noticed that the general trend in the relative properties in the as-built and heat-treated samples are almost in line with the Ashby-Gibson model, with lower values for relative Young's modulus and higher values for the relative UCS of as-built and heat treated lattice than Ashby-Gibson model.

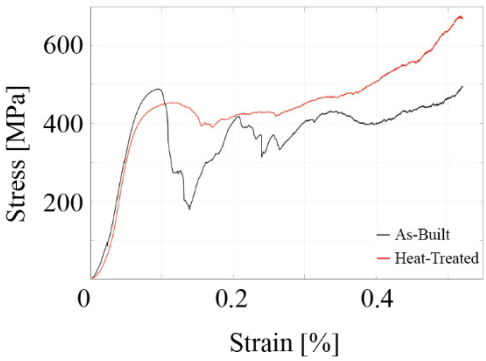

Fig. 6. Compressive deformation behavior of Ti-6Al-4V cellular before and after the heat treatment (cell size 4 mm).

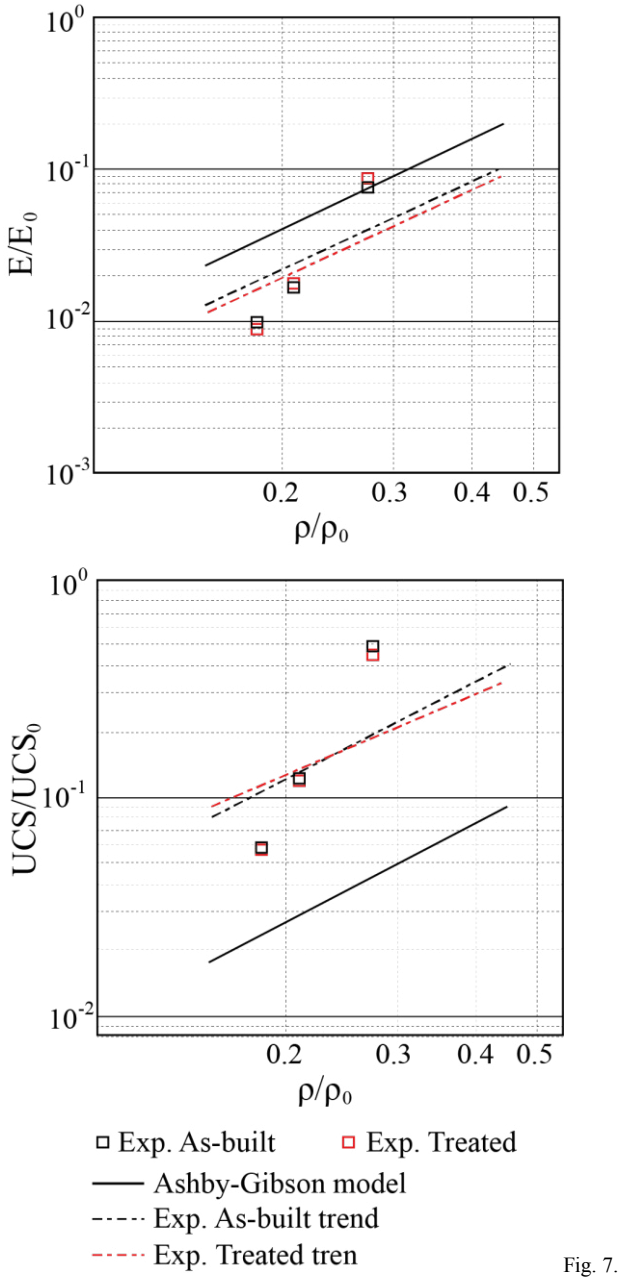

Fig. 7.
Fig. 7 Relative Young's Modulus vs. relative density, and relative UCS vs. relative density.

4. Conclusion

In this research, the effect of the cell size and heat treatment on the compressive strength of the Ti-6Al-4V cellular structures manufactured by EBM was studied. With as-built as well as heat treated samples, two different microstructural conditions were considered.

The main results can be summarized as follows:

1. The as-built microstructure of Ti-6Al-4V alloy which is produced by EBM which is lamellar, with fine α platelets oriented in various directions and heat treatment induces coarser α lamellae.
2. The compressive behavior of the heat-treated sample seems to be rather ductile instead of brittle behavior in as-build condition.
3. In comparison with the heat-treated lattice, the as-built samples bear higher maximum stresses before a steep drop occurs at strains of about 6-7%.
4. In all conditions, by increasing the cell size, the compressive strength of the Ti-6Al-4V cellular structures manufactured by EBM decreases significantly.
5. The trend of relative Young's modulus and relative UCS vs relative density of lattice structures before and after the heat treatment are similar to the Ashby-Gibson model.

References

[1] Standard, A., F2792-12a: Standard Terminology for Additive Manufacturing Technologies (ASTM International, West Conshohocken, PA, 2012). P. Jain, AM Kuthe, Feasibility study of manufacturing using rapid prototyping: FDM approach, Procedia Eng, 2013. **63**: p. 4-11.

[2] Saboori, A., D. Gallo, S. Biamino, P. Fino,M. Lombardi, An overview of additive manufacturing of titanium components by directed energy deposition: Microstructure and mechanical properties. Applied Sciences, 2017. **7**(9): p. 883.

[3] Gibson, I., D.W. Rosen,B. Stucker, Additive manufacturing technologies. Vol. 17. 2014: Springer.

[4] Calignano, F., M. Galati, L. Iuliano,P. Minetola, Design of Additively Manufactured Structures for Biomedical Applications: A Review of the Additive Manufacturing Processes Applied to the Biomedical Sector. Journal of healthcare engineering, 2019. **2019**.

[5] Lindhe, U.,O. Harrysson, Rapid Manufacturing with Electron Beam Melting (EBM)--A Manufacturing Revolution? 2000: Society of Manufacturing Engineers.

[6] Galati, M.,L. Iuliano, A literature review of powder-based electron beam melting focusing on numerical simulations. Additive Manufacturing, 2018. **19**: p. 1-20.

[7] Galati, M., A. Snis,L. Iuliano, Experimental validation of a numerical thermal model of the EBM process for Ti6Al4V. Computers & Mathematics with Applications, 2018.

[8] Mitchell, A., Melting, casting and forging problems in titanium alloys. Materials Science and Engineering: A, 1998. **243**(1-2): p. 257-262.

[9] Weiwei, H., J. Wenpeng, L. Haiyan, T. Huiping, K. Xinting,H. Yu, Research on preheating of titanium alloy powder in electron beam melting technology. Rare Metal Materials and Engineering, 2011. **40**(12): p. 2072-2075.

[10] Fleck, N., V. Deshpande,M. Ashby, Micro-architectured materials: past, present and future. Proceedings of the Royal Society A: Mathematical, Physical and Engineering Sciences, 2010. **466**(2121): p. 2495-2516.

[11] Evans, A.G., J. Hutchinson,M. Ashby, Multifunctionality of cellular metal systems. Progress in materials science, 1998. **43**(3): p. 171-221.

[12] Murr, L., S. Gaytan, F. Medina, H. Lopez, E. Martinez, B. Machado, D. Hernandez, L. Martinez, M. Lopez,R. Wicker, Next-generation biomedical implants using additive manufacturing of complex, cellular and functional mesh arrays. Philosophical Transactions of the Royal Society A: Mathematical, Physical and Engineering Sciences, 2010. **368**(1917): p. 1999-2032.

[13] Niinomi, M., Recent metallic materials for biomedical applications. Metallurgical and materials transactions A, 2002. **33**(3): p. 477.

[14] Park, J.-W., H.-K. Kim, Y.-J. Kim, J.-H. Jang, H. Song,T. Hanawa, Osteoblast response and osseointegration of a Ti–6Al–4V alloy implant incorporating strontium. Acta biomaterialia, 2010. **6**(7): p. 2843-2851.

[15] Ashby, M., The properties of foams and lattices. Philosophical Transactions of the Royal Society A: Mathematical, Physical and Engineering Sciences, 2005. **364**(1838): p. 15-30.

[16] Gibson, L.J.,M.F. Ashby, Cellular solids: structure and properties. 1999: Cambridge university press.

[17] Cansizoglu, O., O. Harrysson, D. Cormier, H. West,T. Mahale, Properties of Ti–6Al–4V non-stochastic lattice structures fabricated via electron beam melting. Materials Science and Engineering: A, 2008. **492**(1-2): p. 468-474.

[18] Heinl, P., L. Müller, C. Körner, R.F. Singer,F.A. Müller, Cellular Ti–6Al–4V structures with interconnected macro porosity for bone implants fabricated by selective electron beam melting. Acta biomaterialia, 2008. **4**(5): p. 1536-1544.

[19] van Grunsven, W., E. Hernandez-Nava, G. Reilly,R. Goodall, Fabrication and mechanical characterisation of titanium lattices with graded porosity. Metals, 2014. **4**(3): p. 401-409.

[20] Jamshidinia, M., L. Wang, W. Tong,R. Kovacevic, The bio-compatible dental implant designed by using non-stochastic porosity produced by Electron Beam Melting®(EBM). Journal of Materials Processing Technology, 2014. **214**(8): p. 1728-1739.

[21] Xiao, L., W. Song, C. Wang, H. Liu, H. Tang,J. Wang, Mechanical behavior of open-cell rhombic dodecahedron Ti–6Al–4V lattice structure. Materials Science and Engineering: A, 2015. **640**: p. 375-384.

[22] Li, S., L.E. Murr, X. Cheng, Z. Zhang, Y. Hao, R. Yang, F. Medina,R. Wicker, Compression fatigue behavior of Ti–6Al–4V mesh arrays fabricated by electron beam melting. Acta Materialia, 2012. **60**(3): p. 793-802.

[23] Murr, L., S. Gaytan, F. Medina, E. Martinez, J. Martinez, D. Hernandez, B. Machado, D. Ramirez,R. Wicker, Characterization of Ti–6Al–4V open cellular foams fabricated by additive manufacturing using electron beam melting. Materials Science and Engineering: A, 2010. **527**(7-8): p. 1861-1868.

[24] Mortensen, A., Y. Conde, A. Rossoll,C. San Marchi, Scaling of conductivity and Young's modulus in replicated microcellular materials. Journal of materials science, 2013. **48**(23): p. 8140-8146.

[25] Tammas-Williams, S., P. Withers, I. Todd,P. Prangnell, Porosity regrowth during heat treatment of hot isostatically pressed additively manufactured titanium components. Scripta Materialia, 2016. **122**: p. 72-76.

[26] Sun, Y., S. Gulizia, C. Oh, D. Fraser, M. Leary, Y. Yang,M. Qian, The influence of as-built surface conditions on mechanical properties of Ti-6Al-4V additively manufactured by selective electron beam melting. Jom, 2016. **68**(3): p. 791-798.

[27] Hernández-Nava, E., C. Smith, F. Derguti, S. Tammas-Williams, F. Léonard, P. Withers, I. Todd,R. Goodall, The effect of defects on the mechanical response of Ti-6Al-4V cubic lattice structures fabricated by electron beam melting. Acta Materialia, 2016. **108**: p. 279-292.

[28] Popov, V., A. Katz-Demyanetz, A. Garkun, G. Muller, E. Strokin,H. Rosenson, Effect of hot isostatic pressure treatment on the electron-beam melted Ti-6Al-4V specimens. Procedia Manufacturing, 2018. **21**: p. 125-132.

[29] Zhai, Y., H. Galarraga,D.A. Lados, Microstructure evolution, tensile properties, and fatigue damage mechanisms in Ti-6Al-4V alloys fabricated by two additive manufacturing techniques. Procedia Engineering, 2015. **114**: p. 658-666.